Anisotropic Transport Properties of Complex Metallic Alloys*

Ana Smontara[a,**] and Janez Dolinšek[b,c]

[a]*Laboratory for the Physics of Transport Phenomena, Institute of Physics, Bijenička c. 46, HR-10000 Zagreb, Croatia*
[b]*Jožef Stefan Institute, University of Ljubljana, Jamova 39, SI-1000 Ljubljana, Slovenia*
[c]*Faculty of Mathematics and Physics, University of Ljubljana, Jadranska 19, SI-1000 Ljubljana, Slovenia*

Abstract. Anisotropic transport properties (electrical resistivity, ρ, and thermal conductivity, κ) of the Y-phase Al-Ni-Co, o-Al$_{13}$Co$_4$ and Al$_4$(Cr,Fe) complex metallic alloys were investigated. They belong to the class of decagonal approximant phases with stacked-layer crystallographic structure and allowed us to study the evolution of anisotropic transport properties with increasing structural complexity and the unit cell size.

Keywords: electrical resistivity, thermal conductivity, anisotropy, Y-Al-Ni-Co, o-Al$_{13}$Co$_4$, Al$_4$(Cr,Fe), complex metallic alloys

INTRODUCTION

The anisotropic crystalline structures of complex metallic alloys (CMAs) result in anisotropic physical properties, when measured along different crystallographic directions. Interesting classes of CMA compounds are the Al$_4$TM (TM = transition metal) and Al$_{13}$TM$_4$ families of intermetallics, which are periodic approximants to the decagonal quasicrystals (d-QCs). Their structures can be viewed as a stacking of atomic planes and this structural anisotropy is at the origin of the anisotropic physical properties. While the stacked-layer crystallographic structure is a common property of the Al$_4$TM and Al$_{13}$TM$_4$ families, member compounds differ in the unit cell size and the number of atomic layers in the unit cell.

In the following we present a study of the anisotropic transport properties (electrical resistivity, ρ, and thermal conductivity, κ) of stacked-layers three CMAs of systematically increasing structural complexity comprising two, four and six atomic layers in the unit cell. The first one is the Al$_{76}$Co$_{22}$Ni$_2$ compound,[1,2] known as the Y-phase of Al-Ni-Co, which belongs to the Al$_{13}$TM$_4$ class and is a monoclinic approximant to the decagonal phase with two atomic layers within one periodic unit of $\approx$ 0.4 nm along the stacking direction and a relatively small unit cell, comprising 32 atoms. The second compound studied is the orthorhombic o-Al$_{13}$Co$_4$ compound,[3] belonging to the same Al$_{13}$TM$_4$ class of decagonal approximants with four atomic layers within one

periodic unit of $\approx$ 0.8 nm along the stacking direction and a unit cell comprising 102 atoms. The third one is the Al$_4$(Cr,Fe) complex metallic alloy with composition Al$_{80}$Cr$_{15}$Fe$_5$,[4,5] belonging to the class of orthorhombic Al$_4$TM phases, which are approximants to the decagonal phase, with six atomic layers in a periodic unit of 1.25 nm and 306 atoms in the giant unit cell. The above selection of samples allowed us to consider the evolution of anisotropic transport properties of the stacked-layer CMAs with increasing structural complexity and the unit cell size.

STRUCTURAL CONSIDERATION AND SAMPLE PREPARATION

The Y-Al-Ni-Co phase is in literature described as the Al$_{13-x}$(Co$_{1-y}$Ni$_y$)$_4$ monoclinic phase,[6] belonging to the Al$_{13}$TM$_4$ class of decagonal approximants. The structure of Al$_{13-x}$(Co$_{1-y}$Ni$_y$)$_4$ with x = 0.9 and y = 0.12, cor-responding to composition Al$_{75}$Co$_{22}$Ni$_3$, was first described by Zhang *et al.*[6] Lattice parameters of the monoclinic unit cell are a = 1.7071 nm, b = 0.40993 nm, c = 0.74910 nm, β = 116.17 °, with 32 atoms in the unit cell. The structure of the Al$_{13-x}$(Co$_{1-y}$Ni$_y$)$_4$ is built up of one type of flat atomic layers, which are related to each other by a 2_1 axis, giving $\approx$ 0.4 nm period along the [0 1 0] stacking direction (corresponding to the periodic direction in the related decagonal d-Al-Ni-Co quasicrystal) and two atomic layers within one periodicity unit. Locally, the structure shows close resemblance to the

---

d-$Al_{70}Co_{15}Ni_5$ quasicrystal,[7] which also consists of only one type of a quasiperiodic layer, repeated by a 10_5 axis and giving the same ≈ 0.4 nm period.

The orthorhombic o-$Al_{13}Co_4$ phase is another member of the $Al_{13}TM_4$ class of decagonal approximants. According to the structural model by Grin *et al.*,[8] lattice parameters of the o-$Al_{13}Co_4$ orthorhombic unit cell are $a = 0.8158$ nm, $b = 1.2342$ nm and $c = 1.4452$ nm with 102 atoms in the unit cell. The structure corresponds to a four-layer stacking along [1 0 0],[6,8] with flat layers at $x = 0$ and $x = 1/2$ and two symmetrically equivalent puckered layers at $x = 1/4$ and $3/4$, giving ≈ 0.8 nm period along [1 0 0].

The $Al_4(Cr,Fe)$ phase[9] belongs to the Al_4TM class of body-centered orthorhombic phases. Their structure can be described as a periodic repetition of a sequence P'FPp'fp of six atomic layers stacked within one periodicity length of 1.25 nm along a, showing close structural relationship to the six-layer Al-TM d-QCs with the same periodicity. The block P'FP is composed of a flat layer F at $x = 0$ and a puckered layer P at $x \approx a/6$, whereas the puckered layer P' is in mirror-reflecting position across the F layer. The block p'fp equals the block P'FP translated by ($a/2$, $b/2$, $c/2$). The composition of our sample was $Al_{80}Cr_{15}Fe_5$ and its structure could be assigned to the orthorhombic phase, previously described by Deng *et al.*,[9] with unit cell parameters $a = 1.2500$ nm, $b = 1.2617$ nm, $c = 3.0651$ nm and 306 atoms in the giant unit cell.

The single crystals used in our study were grown from an incongruent Al-rich melt of required composition by the Czochralski method[10] using a native seed. In order to perform crystallographic-direction-dependent studies, we have cut from the ingot three bar-shaped samples of average dimensions $2 \times 2 \times 7$ mm³. For the monoclinic samples $Al_{76}Co_{22}Ni_2$, (abbreviated as Y-Al-Ni-Co in the following) the long axes were along three orthogonal directions. The long axis of the first sample was along the [0 1 0] stacking direction (designated in the following as b), which corresponds to the periodic direction in the related d-Al-Ni-Co quasicrystal. The (a,c) monoclinic plane corresponds to the quasiperiodic plane in d-QCs and the second one was cut with its long axis along [0 0 1] (c) direction, whereas the third one was cut along the direction perpendicular to the (b,c) plane. This direction is designated as a^* (it lies in the monoclinic plane at an angle 26° with respect to a and perpendicular to c). For orthorhombic o-$Al_{13}Co_4$ and body-centered $Al_{87}Cr_7Fe_6$ the long axes were along the three crystallographic directions of the orthorhombic unit cell. The [1 0 0] stacking direction (designated in the following as a) corresponds to the periodic direction in d-QCs, whereas the [0 1 0] (b) and [0 0 1] (c) directions lie within the atomic planes (corresponding to the quasiperiodic directions in d-QCs).
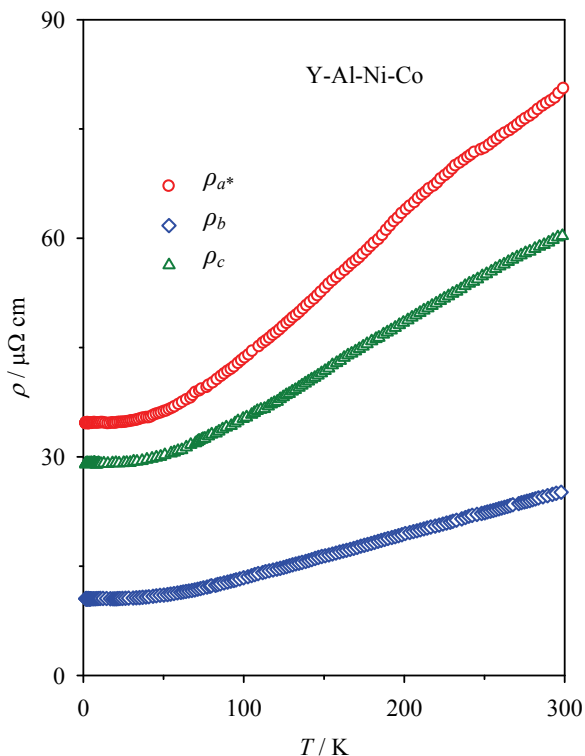
Figure 1. Temperature-dependent electrical resistivity, $\rho(T)$, of Y-Al-Ni-Co along three orthogonal crystallographic directions a^*, b and c.

ANISOTROPIC ELECTRICAL RESISTIVITY

Electrical resistivity, $\rho(T)$, was measured from 2 K to 300 K using the standard four-terminal technique. The $\rho(T)$ data of all the three complex metallic alloys for the three crystallographic directions are displayed in Figures 1, 2 and 3, respectively.

The resistivity of Y-Al-Ni-Co is the lowest along the b direction perpendicular to the atomic planes, where its room temperature (r.t.) value amounts $\rho_b^{r.t.} = 25$ $\mu\Omega$ cm and the residual resistivity is $\rho_b^{2 K} = 10$ $\mu\Omega$ cm. The two in-plane resistivities are higher, amounting $\rho_c^{r.t.} = 60$ $\mu\Omega$ cm and $\rho_c^{2 K} = 29$ $\mu\Omega$ cm for the c direction and $\rho_{a^*}^{r.t.} = 81$ $\mu\Omega$ cm and $\rho_{a^*}^{2 K} = 34$ $\mu\Omega$ cm for the a^* direction. While ρ_b is considerably smaller than ρ_{a^*} and ρ_c by a factor of about 3, the two in-plane resistivities are much closer, $\rho_{a^*}/\rho_c \approx 1.3$. The above resistivity values, appearing in the order $\rho_b < \rho_c < \rho_{a^*}$ (even the inequality $\rho_b << \rho_c < \rho_{a^*}$ considered to hold), reveal that Y-Al-Ni-Co is a good electrical conductor along all three crystallographic directions. The ratios of the resistivities ρ_i/ρ_j along different crystallographic directions vary little over the whole investigated temperature range $2-300$ K, amounting $\rho_{a^*}/\rho_b \approx 3.2$, $\rho_c/\rho_b \approx 2.5$ and $\rho_{a^*}/\rho_c \approx 1.3$. The strong positive temperature coefficient (PTC) of the resistivity along all three crystallographic directions demonstrates predominant role of the electron-phonon
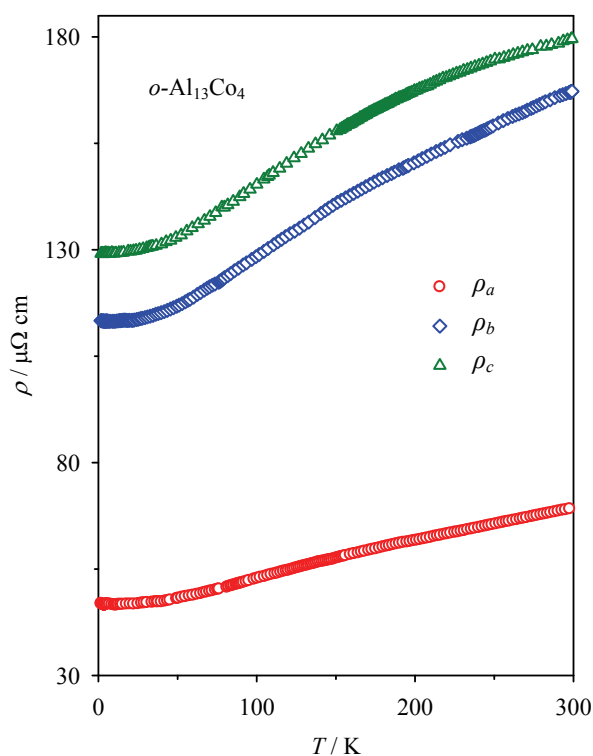
Figure 2. Temperature-dependent electrical resistivity, $\rho(T)$, of o-Al$_{13}$Co$_4$ along three orthogonal crystallographic directions a, b and c.

Figure 3. Temperature-dependent electrical resistivity, $\rho(T)$, of Al$_{80}$Cr$_{15}$Fe$_5$ along the three crystallographic directions a, b and c.

scattering mechanism, so that the resistivity is of the Boltzmann type.

The resistivity of o-Al$_{13}$Co$_4$ (Figure 2) is again the lowest along the stacking a direction perpendicular to the atomic planes, where its room temperature value amounts $\rho_a^{\text{r.t.}} = 69$ µΩ cm and the residual resistivity is $\rho_a^{2\,K} = 47$ µΩ cm. The two in-plane resistivities are higher, amounting $\rho_b^{\text{r.t.}} = 169$ µΩ cm and $\rho_b^{2\,K} = 113$ µΩ cm for the b direction and $\rho_c^{\text{r.t.}} = 180$ µΩ cm and $\rho_c^{2\,K} = 129$ µΩ cm for the c direction. The anisotropy of the two in-plane resistivities is small, amounting at room temperature to $\rho_c^{\text{r.t.}} / \rho_b^{\text{r.t.}} = 1.07$, whereas the anisotropy to the stacking direction is considerably larger, $\rho_c^{\text{r.t.}} / \rho_a^{\text{r.t.}} = 2.6$ and $\rho_b^{\text{r.t.}} / \rho_b^{\text{r.t.}} = 2.5$. The anisotropic resistivities thus appear in the order $\rho_a < \rho_b < \rho_c$ (the inequality $\rho_a \ll \rho_b < \rho_c$ may be written). The PTC of the resistivity along all three crystallographic directions as for the Y-Al-Ni-Co demonstrates predominant role of the electron–phonon scattering mechanism and the resistivity is of Boltzmann type.

As in two previous examples, the resistivity in Al$_{80}$Cr$_{15}$Fe$_5$ (Figure 3.) is the lowest along the stacking a direction perpendicular to the atomic planes. ρ_a shows a PTC in the whole investigated temperature interval and a room temperature value $\rho_a^{\text{r.t.}} = 297$ µΩ cm. The resistivities within the atomic planes (which correspond to the aperiodic planes in d-QC's) are higher and exhibit

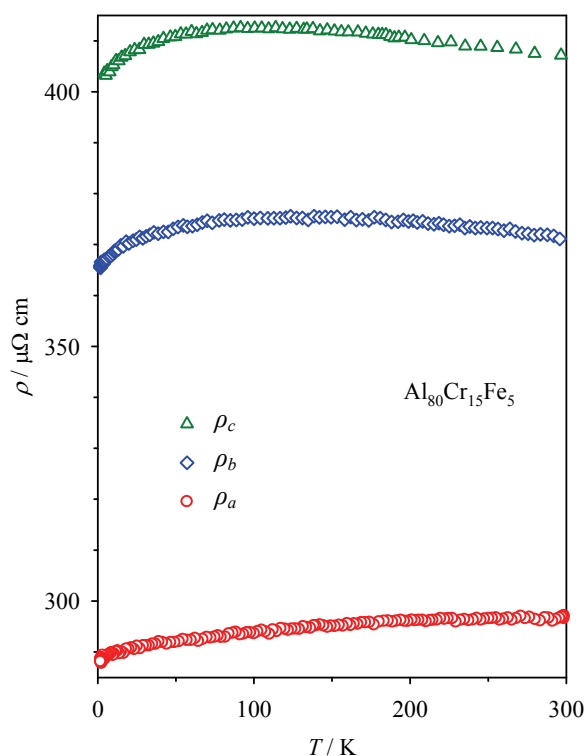qualitatively different temperature-dependencies with a broad maximum, where the temperature coefficient is reversed. ρ_a exhibits a maximum at about 125 K with the peak value 375 µΩ cm and the room temperature value $\rho_a^{\text{r.t.}} = 371$ µΩ cm. The resistivity ρ_c is the highest; its maximum value 413 µΩ cm occurs at 100 K and the room temperature value is $\rho_c^{\text{r.t.}} = 407$ µΩ cm. At room temperature, the ratios of the resistivities amount $\rho_c / \rho_a = 1.37$, $\rho_b / \rho_a = 1.25$ and $\rho_c / \rho_b = 1.10$. The resistivity of Al$_{80}$Cr$_{15}$Fe$_5$ is thus qualitatively different from the Boltzmann-type PTC resistivities of Y-Al-Ni-Co and o-Al$_{13}$Co$_4$, and is described by the theory of the slow charge carriers.[11]

ANISOTROPIC THERMAL CONDUCTIVITY

Thermal conductivity was measured between 2 and 300 K using an absolute steady-state heat-flow method. The thermal flux through the samples was generated by a 1 kΩ RuO$_2$ chip-resistor, glued to one end of the sample, while the other end was attached to a copper heat sink. The temperature gradient across the sample was monitored by a chromel-gold differential thermo-couple (gold with the fraction of iron atoms of 0.07 %). The total thermal conductivity κ of Y-Al-Ni-Co, o-Al$_{13}$Co$_4$ and AlCrFe along the three crystallographic directions is displayed in the upper panel of Figures 4–6.
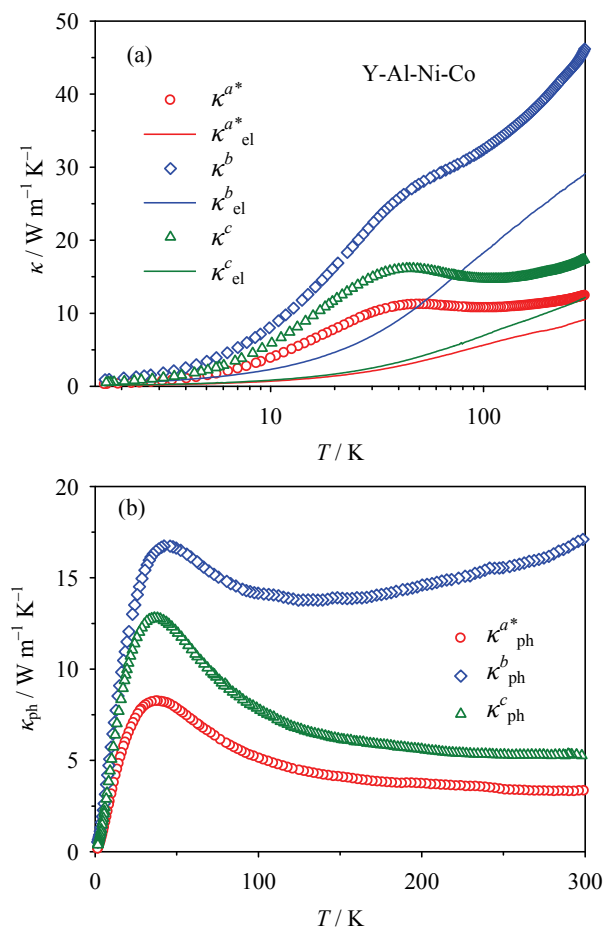
Figure 4. (a) Thermal conductivity, $\kappa(T)$, of Y-Al-Ni-Co along the three crystallographic directions a^*, b and c. Electronic contributions $\kappa_{el}(T)$, estimated from the Wiedemann-Franz law, are shown by solid curves. (b) Phononic thermal conductivity $\kappa_{ph}(T) = \kappa(T) - \kappa_{el}(T)$ along the three crystallographic directions.

Figure 5. (a) Total thermal conductivity, $\kappa(T)$, of o-Al$_{13}$Co$_4$ along the three crystallographic directions a, b and c. Electronic contributions, $\kappa_{el}(T)$, estimated from the Wiedemann-Franz law, are shown by solid curves. (b) Phononic thermal conductivity $\kappa_{ph}(T) = \kappa(T) - \kappa_{el}(T)$ along the three crystallographic directions.

The phononic contribution $\kappa_{ph} = \kappa - \kappa_{el}$ was estimated by subtracting the electronic contribution κ_{el} (shown by solid curves in the upper panel of Figures 4–6.) from the total conductivity using the Wiedemann-Franz law, $\kappa_{el} = \pi^2 k_B^2 T \sigma(T)/3 e^2$ and the measured electrical conductivity data $\sigma(T) = \rho^{-1}(T)$ from Figures 1–3. Though the use of the Wiedemann-Franz law is a rough approximation, in this way determined κ_{ph} (shown in the lower panel of Figures 4–6) gives an indication of the anisotropy of the phononic spectrum.

In Y-Al-Ni-Co at room temperature, we get the following anisotropy: $\kappa^{a^*} = 12.5$ W/m K , $\kappa_{el}^{a^*} = 9.1$ W/m K with their ratio $(\kappa_{el}^{a^*}/\kappa^{a^*})_{r.t.} = 0.73$, $\kappa^b = 46.3$ W/m K, $\kappa_{el}^b = 29.2$ W/m K with $(\kappa_{el}^b/\kappa^b)_{r.t.} = 0.63$ and $\kappa^c = 17.4$ W/m K, $\kappa_{el}^c = 12.2$ W/m K with $(\kappa_{el}^c/\kappa^c)_{r.t.} = 0.70$. Electrons are thus majority heat carriers at room temperature for all three directions. The anisotropic thermal conductivities appear in the order $\kappa^{a^*} < \kappa^c < \kappa^b$ and similarly $\kappa_{el}^{a^*} < \kappa_{el}^c < \kappa_{el}^b$, which is identical to the
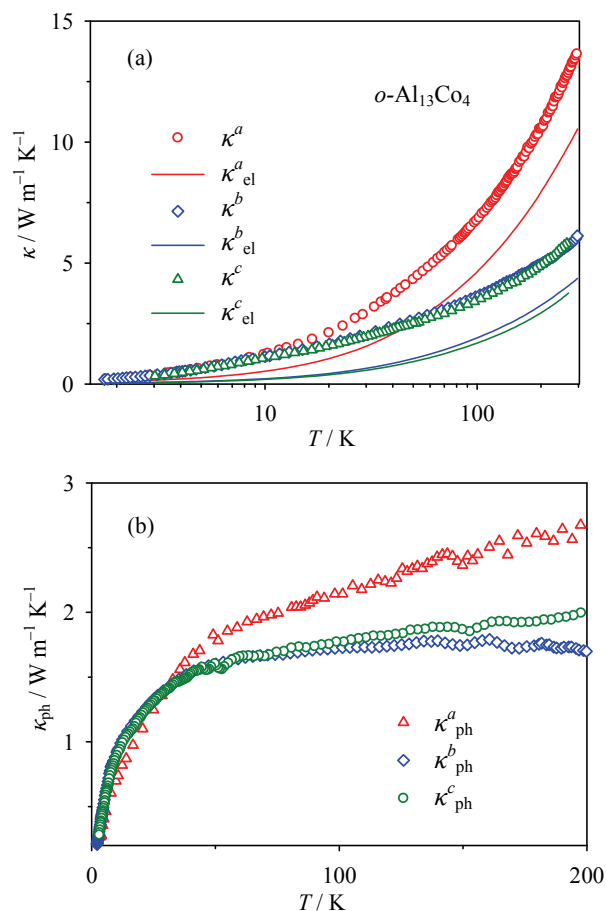
order in which the anisotropic electrical conductivities of Y-Al-Ni-Co appear (Figure 1): $\sigma_{a^*} < \sigma_c < \sigma_b$. The phononic thermal conductivity is shown in the lower panel of Figure 6. We observe that anisotropic κ_{ph}'s again appear in the same order, $\kappa_{ph}^{a^*} < \kappa_{ph}^c < \kappa_{ph}^b$, so that the phononic conductivity is the highest along the b direction perpendicular to the (a,c) atomic layers, whereas the two in-plane conductivities are lower and show smaller anisotropy. For all directions, κ_{ph}'s show a typical phonon *umklapp* maximum at about 40 K. The above results show that Y-Al-Ni-Co is the best conductor for both the electricity and heat along the stacking b direction, whereas both conductivities are smaller in the (a,c) plane.

In Al$_{13}$Co$_4$ at room temperature (r.t.), we get the following anisotropy: $\kappa^a = 12.5$ W / m K, $\kappa_{el}^a = 10.2$ W / m K with their ratio $(\kappa_{el}^a / \kappa^a)_{r.t.} = 0.82$, $\kappa^b = 6.1$ W / m K, $\kappa_{el}^b = 4.4$ W / m K with $(\kappa_{el}^b / \kappa^b)_{r.t.} = 0.72$ and $\kappa^c = 6.2$ W / m K, $\kappa_{el}^c = 4.1$ W / m K with $(\kappa_{el}^c / \kappa^c)_{r.t.} = 0.66$.
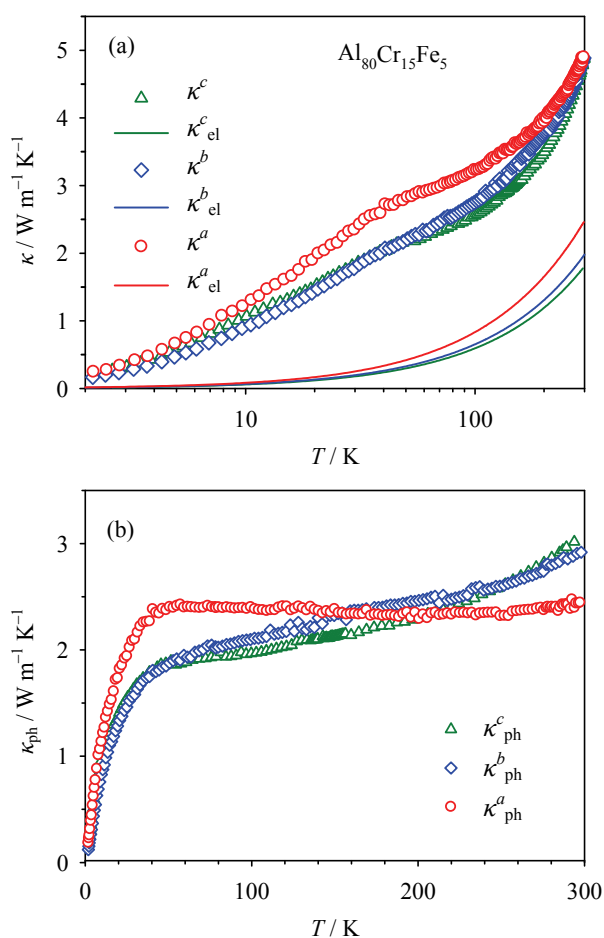
Figure 6. (a) Total thermal conductivity, $\kappa(T)$, of $Al_{80}Cr_{15}Fe_5$ along the three crystallographic directions a, b and c of the orthorhombic unit cell. Electronic contributions, $\kappa_{el}(T)$, estimated from the Wiedemann-Franz law, are shown by solid curves. (b) Phononic thermal conductivity $\kappa_{ph}(T) = \kappa(T) - \kappa_{el}(T)$ along the three crystallographic directions.

Charge carriers are thus majority heat carriers at room temperature for all three directions. The anisotropic thermal conductivities appear in the order $\kappa^c \approx \kappa^b < \kappa^a$, and the same order applies to the electronic parts $\kappa_{el}^{\ c} \approx \kappa_{el}^{\ b} < \kappa_{el}^{\ a}$. The thermal conductivity is thus the highest along the stacking a direction, whereas the in-plane conductivity is smaller with no noticeable anisotropy between the two in-plane directions b and c. Figure 2 shows that as in Y-Al-Ni-Co the electrical conductivity of o-$Al_{13}Co_4$ is also the highest along a (appearing in the order $\sigma_c < \sigma_b < \sigma_a$). The phononic thermal conductivity is shown in the lower panel of Figure 6. We observe that the anisotropy of κ_{ph} is small and no systematic differences between the three directions can be claimed unambiguously.

Both κ and κ_{el} in the $Al_{80}Cr_{15}Fe_5$ are again the highest along the stacking a direction, and the anisotropy between the two in-plane (b,c) conductivities is

small. The phononic contribution $\kappa_{ph} = \kappa - \kappa_{el}$ is shown in the lower panel of Figure 6, where we observe that the conductivity $\kappa_{ph}^{\ a}$ along the a direction in the low-temperature regime below 50 K (which can be associated with the regime where *umklapp* processes are still ineffective) is the highest, whereas the two in-plane conductivities $\kappa_{ph}^{\ b}$ and $\kappa_{ph}^{\ c}$ are somewhat smaller and also show very weak in-plane anisotropy.

CONCLUSIONS

Electrical resistivities of the investigated Y-Al-Ni-Co, o-$Al_{13}Co_4$ and $Al_4(Cr,Fe)$ show similar anisotropy, being weak for the two in-plane directions and stronger between in-plane to the stacking direction. For all three compounds, the resistivity is the lowest along the stacking direction. The resistivity values are increasing with increasing complexity of the compounds, being the lowest for the Y-Al-Ni-Co, significantly higher for the o-$Al_{13}Co_4$ and even higher for the $Al_4(Cr,Fe)$. This overall increase of the resistivity is also accompanied by the change of the temperature coefficient: while the resistivities of Y-Al-Ni-Co and o-$Al_{13}Co_4$ show Boltzmann-type PTC for all crystallographic directions, the temperature-dependent in-plane resistivity of $Al_4(Cr,Fe)$ is non-Boltzmann, exhibiting a maximum by changing the slope from PTC to NTC, whereas the resistivity along the stacking direction still shows PTC in the investigated temperature range.

The thermal conductivity of the Y-Al-Ni-Co, o-$Al_{13}Co_4$ and $Al_4(Cr,Fe)$ behaves in complete analogy to the electrical resistivity, by showing weak in-plane anisotropy and considerable anisotropy to the stacking direction. For all three compounds, the thermal conductivity is the highest along the stacking direction, so that the investigated decagonal approximant phases are the best conductors for both the electricity and heat along the stacking direction perpendicular to the atomic planes. At room temperature, Y-Al-Ni-Co shows the highest thermal conductivity, and $Al_4(Cr,Fe)$ the lowest one, indicating that increased complexity of the structure results in less efficient electronic and phononic transport of the heat.

REFERENCES

1. A. Smontara, I. Smiljanić, J. Ivkov, D. Stanić, O. S. Barišić, Z. Jagličić, P. Gille, M. Komelj, P. Jeglič, M. Bobnar, and J. Dolinšek, *Phys. Rev. B* **78** (2008) 104204-1–104204-13.
2. M. Komelj, J. Ivkov, A. Smontara, P. Gille, P. Jeglič, and J. Dolinšek, *Solid State Commun.* **149** (2009) 515–518.
3. J. Dolinšek, M. Komelj, P. Jeglič, S. Vrtnik, D. Stanić, P. Popčević, J. Ivkov, A. Smontara, Z. Jagličić, P. Gille, and Yu. Grin, *Phys. Rev. B* **79** (2009) 184201-1–184201-12.
4. J. Dolinšek, P. Jeglič, M. Komelj, S. Vrtnik, A. Smontara, I. Smiljanić, A. Bilušić, J. Ivkov, D. Stanić, E. S. Zijlstra, B. Bauer, and P. Gille, *Phys. Rev. B* **76** (2007) 174207-1–174207-13.
5. J. Dolinšek, S. Vrtnik, A. Smontara, M. Jagodič, Z. Jagličić, B. Bauer, and P. Gille, *Phil. Mag.* **88** (2008) 2145–2153.
6. B. Zhang, V. Gramlich, and W. Steurer, *Z. Kristallogr.* **210** (1995) 498–503.
7. W. Steurer, T. Haibach, B. Zhang, S. Kek, and R. Lück, *Acta Crystallogr. B* **49** (1993) 661–675.
8. J. Grin, U. Burkhardt, M. Ellner, and K. Peters, *J. Alloys Compd.* **206** (1994) 243–247.
9. D. W. Deng, Z. M. Mo, and K. H. Kuo, *J. Phys.: Condens. Matter* **16** (2004) 2283–2296.
10. P. Gille and B. Bauer, *Cryst. Res. Technol.* **43** (2008) 1161–1167.
11. G. T. de Laissardière, J.-P. Julien, and D. Mayou, *Phys. Rev. Lett.* **97** (2006) 026601-1–026601-4.

SAŽETAK

Anizotropna transportna svojstva kompleksnih metalnih legura

Ana Smontara[a] i Janez Dolinšek[b,c]

[a]*Laboratorij za fiziku transportnih svojstava, Institut za fiziku, Bijenička 46, HR-10000 Zagreb, Hrvatska*
[b]*Jožef Stefan Institute, University of Ljubljana, Jamova 39, SI-1000 Ljubljana, Slovenia*
[c]*Faculty of Mathematics and Physics, University of Ljubljana, Jadranska 19, SI-1000 Ljubljana, Slovenia*

Prikazana su istraživanja anizotropnih transportnih svojstava (električne otpornosti, ρ, i toplinske vodljivosti, κ) kompleksnih metalnih legura Y-Al-Ni-Co, o-Al$_{13}$Co$_4$ i Al$_4$(Cr,Fe). Navedene legure pripadaju klasi aproksimanata dekagonalne faze, karakterizirane *"stacked-layer"* kristalnom strukturom, te su pogodne za ispitivanje utjecaja složenosti kristalne strukture i veličine jedinične ćelije na transportna svojstva.